Desalination and Water Treatment
www.deswater.com
doi: 10.5004/dwt.2022.28129

248 (2022) 1–17
February

Effect of the variation of a mass-flow-rate and a number of collectors on the performance of an active solar still

Devesh Kumar[a], R.K. Sharma[b], Desh Bandhu Singh[c,*]

[a]*Department of Mechanical Engineering, Madan Mohan Malviya University of Technology, Gorakhpur - 273010, U.P., India, email: dkme@mmmut.ac.in*
[b]*University of Petroleum and Energy Studies (UPES), Bidholi, Premnagar, Dehradun – 248007, Uttarakhand, India, email: ram.sharma@upes.ac.in*
[c]*Department of Mechanical Engineering, Graphic Era Deemed to be University, Bell Road, Clement Town, Dehradun – 248002, Uttarakhand, India, email: dbsiit76@gmail.com/deshbandhusingh.me@geu.ac.in*

Received 1 July 2021; Accepted 28 December 2021

ABSTRACT

This work focuses on the effect of dissimilarity of mass flow rate ($\dot{m}_f$) and number of collectors (N) on overall yearly energy as well as exergy for single slope solar still included with N similar partially covered PV/T flat plate collectors (NPVTFPC-SS) in which collectors are series connected. The water depth has been taken as 0.14 m. The proposed analysis consists of four weather conditions for New Delhi complex climate. The different parameters have been estimated by feeding all relevant equations to mathematical programming done in MATLAB-2015a. The estimation of different parameters has been carried out by varying $\dot{m}_f$ and N while keeping water depth as constant for knowing the effect of dissimilarity of $\dot{m}_f$ and N on yearly overall energy and exergy for NPVTFPC-SS. It has been concluded that the value of yearly overall energy and exergy for NPVTFPC-SS having series connection at given value of water depth of 0.14 m increases with the increase in N at given $\dot{m}_f$; however, they have been found to decrease with the increase in $\dot{m}_f$ at given N. Furthermore, overall energy and exergy have been found to be almost constant beyond $\dot{m}_f$ value of 0.1 m at given N. The performance of NPVTFPC-SS has been compared with the performance of similar system without PV/T.

Keywords: Annual energy; Annual exergy; Mass flow rate; N; Active solar still

1. Introduction

The investigation of solar still of single slope type by incorporating solar collectors for yearly fresh water yielding, energy and exergy is the need of time as the world is facing with the scarcity of fresh water. Solar energy based water purifier has the potential to mitigate the contemporary issue of fresh water scarcity. At the same time, these types of devices are environment friendly as no pollutants are emitted. The conventional source of energy is detrimental to the environment due to the emission of green house gases and hence to the human beings and the source of conventional energy is limited, too. The active solar still involving solar panel can generate DC electric power as well as fresh water. This type of active solar still is self-sustainable and hence, it can be installed and operated successfully at the remote locations where sunlight is present in abundance. Yearly overall energy as well as exergy analysis of solar still is essential because it gives an idea about technically feasibility of the system from energy and exergy viewpoints.

The active solar still came into existence in 1983 [1] and from that time, many new designs have been reported by

* Corresponding author.

various researchers around the globe. The active solar still means the provision of external source of heat to the basin of passive type solar still. The external source of heat can be made available as solar collectors/industry waste heat using heat exchanger or similar other kinds of provision can be made. Rai and Tiwari [1] reported the enhancement in yield of active solar still by incorporating one conventional flat plate collector (FPC) over passive type solar still of the same basin area due to the addition of heat to the basin in active mode of operation. This water purifier was not self-sustainable as the pump needed some electric power for working which was supplied through grid.

The active solar still in the forced mode of operation can be made self-sustainable by incorporating solar panel. Kumar and Tiwari [2] proposed the integration of PV/T with FPC for supplying heat to basin of passive type solar still taking inspiration from the work of Kern and Russell [3]. It was reported by Kern and Russell that the electrical efficiency of solar panel got increased upon integration of solar panel with solar collector due the removal of heat by fluid passing below the panel. Kumar and Tiwari reported the improvement in output by 3.5 times over the similar passive type solar still due to the addition of heat by two collectors in which only one of them was integrated with PV/T for making the system self-sustainable. The work of Kumar and Tiwari was extended by Singh et al. [4] for double slope (DS) type solar still in active mode. Further, Singh et al. [5] and Tiwari et al. [6] reported the experimental investigation of solar still by incorporating two FPCs in which both FPCs were partially integrated with PV/T. They reported an enhancement in DC electrical output; however, the yield of fresh water was less as compared to the system reported by Kumar and Tiwari [2]. The heat gain was less because more area of FPCs was covered by PV/T. Further, active type solar still was studied under optimized situation [7–11]. It was reported that DS type solar still under optimized condition by incorporating N alike PVT-FPCs had 74.66% higher energy payback time (ENPBT) over passive type DS solar still. The value of exergoeconomic parameter for single slope type solar still was found to be 47.37% higher than the passive type of single slope solar still of same basin area. Sahota et al. [12] reported the use of nanofluid in DS type solar still in active mode for enhancing the fresh water output. Carranza et al. [13] have experimentally investigated the performance of DS type solar still loaded with nanofluid by incorporating preheating of saline water and concluded that water yield increases due to better thermophysical properties of nanofluid as compared to base fluid. Kouadri et al. [14] have investigated solar still by incorporating zinc and copper oxides for the location of Algeria and compared the yield with conventional solar still and concluded that the water yield was improved by 79.39% due to having better thermophysical characteristic of nanofluid.

The output of solar still could further be enhanced by changing the design of solar collector which could absorb higher amount of heat from the sun or by changing the design of solar still. PV/T integrated FPC could gain higher heat if some concentrating part was integrated with FPC. With this concept in mind, Atheaya et al. [15] proposed PV/T integrated compound parabolic concentrator collector (CPC) and reported its thermal model which was further extended by Tripathi et al. [16] for N collectors connected in series in which loop was opened. Singh and Tiwari [17–19], Gupta et al. [20,21], Singh et al. [22,23] and Sharma et al. [24] investigated solar still of basin type by incorporating characteristic equations development and concluded that solar still of DS type performs better than solar still of single slope type under optimized conditions of mass flow rate ($\dot{m}_f$) and number of collectors (N) at 0.14 m water depth due to better distribution of solar energy in the case of DS type. Prasad et al. [25], Bharti et al. [26] and Singh [27] investigated solar still of DS type from sensitivity viewpoint and concluded that the sensitivity analysis helps designer and installer of solar systems as which parameter should be focused more for a particular application.

The heat gain by solar collector could further be enhanced by providing evacuated tubes because convection loss does not take place through vacuum. Sampathkumar et al. [28] investigated the solar still by incorporating evacuated tubular collector and reported an increase of 129% over the solar still of the same basin area due to the addition of heat to the basin by collectors. An investigation of solar still in natural mode of operation by incorporating evacuated tubes was done by Singh et al. [29] and reported exergy efficiency lying in the range of 0.15% to 8%. Further, an investigation of solar still incorporated with evacuated tubes was done in forced mode of operation by inserting pump between collector and basin and reported enhanced fresh water output as compared to the similar system operated in natural mode due to better circulation of fluid in the forced mode of operation [30]. Mishra et al. [31] reported characteristic equation development for N alike series connected ETCs. The work reported by Mishra et al. [31] was further extended by Singh et al. [32–34]. The thermal modeling of basin type solar still by incorporating N alike ETCs was reported by them and comparison was also made between single slope active water purifier and DS type solar still in active mode taking energy, exergy, energy metrics, exergoeconomic and enviroeconomic parameters as basis. Issa and Chang [35] further extended the work of singh et al. by connecting ETCs in mixed mode of operation experimentally and reported enhanced output as compared to similar set up in passive mode due to heat addition by collectors in active mode. Moreover, Singh and Al-Helal [36], Singh [37] and Sharma et al. [38,39] reported development of characteristic equations and the observations based on the energy metrics for solar still by incorporating evacuated tubular collector as well as compound parabolic concentrator integrated evacuated tubular collector.

Patel et al. [40–42] have reviewed solar still recently by incorporating different types of collectors and by incorporating various types of collectors to the basin of solar still. They concluded that the performance of solar still depends on the shape of basin liners as well as number of collectors. The evaporation rate gets enhanced by increasing number of collectors and providing improved design of basin liner. Due to enhancement in the rate of evaporation, the better performance of solar still is obtained. Further, Singh et al. [43] reviewed solar still by incorporating different types of collectors and loaded with nanofluid with an aim to find the effect of nanofluid on the performance of active solar

still. Nanofluid is obtained by mixing a small quantity of nanoparticles to water. The effect of adding nanoparticles to water in solar still is to increase the output (potable water and exergy) of solar still. The better performance of nanofluid loaded solar still than loaded with water is due to the possession of better thermo-physical characteristic of nanofluid as compared to water. Bansal et al. [44] have reported the mini review of changing the material of absorber on the performance of solar still. Shankar et al. [45] have studied ETC integrated solar still in natural as well as forced mode and concluded that forced mode is better for environment as higher carbon credit was observed in forced mode due to more addition of heat to basin in the case of forced mode. Abdallah et al. [46] have investigated spherical and pyramid basin solar stills and concluded that the spherical basin solar still gave 57.1% higher water yield due to better utilization of solar radiation in the case of spherical basin.

Thakur et al. [47,48] have studied solar still using different microparticle-coated absorber plate experimentally and they concluded that the daily fresh water yielding was 33.13% higher than conventional solar still due to improved thermo-physical property. They have also studied active solar still by incorporating carbon pellets as energy storage material and conclude that the daily fresh water yielding for the proposed system was 50.21% higher than the conventional solar still. It was reported that fresh water yielding of solar still enhances by 15.6% when condensing surface is coated with nano silicon due to change in condensation pattern from film wise to drop wise [49]. Said et al. [50] have studies the advancement in nanofluid and they have concluded that nano-particles can improve the performance substantially when dispersed uniformly and suspended stably in base fluid. The use of nanofluid in collectors also increases the performance substantially due to improved thermophysical characteristics [51]. Sharma et al. [52] performed experimental validation of DS solar still integrated with ETC and reported a fair agreement between theoretical and experimental values.

From the current literature survey, it is seen that the effect of $\dot{m}_f$ and N on the yearly overall energy as well as exergy of NPVTFPC-SS has not been reported by any researcher throughout the globe. Hence, this research work deals with the investigation of effect of $\dot{m}_f$ and N on the yearly overall energy as well as exergy of NPVTFPC-SS. Four kinds of weather situations have been considered while estimating values of energy and exergy using computer code in MATLAB-2015a. The difference between the earlier reported work and the proposed work lies in the fact that effect of dissimilarities of $\dot{m}_f$ and N on the yearly overall energy as well as exergy has been estimated for NPVTFPC-SS, whereas, in the earlier reported works, yearly overall energy as well as exergy for the active system have been estimated at a particular value of $\dot{m}_f$ and N. Also, the performance of NPVTFPC-SS has been compared with the performance of similar system without PV/T.

2. System metaphors

The schematic diagram of NPVTFPC-SS has been revealed as Fig. 1 and its specification as Table 1. In the proposed NPVTFPC-SS, heat is provided by N similar partially covered PVTFPCs and hence works in active mode. When sunlight falls on the surface of condensing cover, it is transmitted to water surface after reflection and absorption. The transmittivity of the glass is about 0.95. So, major portion of sunlight is transmitted to water surface. Again, after reflection and absorption by water surface, the sunlight is transmitted to blackened surface kept at the bottom of basin where almost all parts of radiation gets absorbed. The temperature of blackened surface kept at the bottom rises and heat is transferred to water from the blackened surface. Water in the basin also receives heat from N alike series connected PV/T collectors. Thus, temperature of water rises, and evaporation occurs which depends on the temperature difference between water surface and inside surface of glass cover. The vapor gets condensed through film wise condensation at the inside surface of glass. The condensed water trickles down under the gravity and gets collected at the channel fixed at the lower side. The fresh water is then collected in jar through tube connected to the channel.

3. Mathematical modeling based on energy balance equations

Mathematical modeling of N similar partially covered NPVTFPC-SS means writing equations for all its components by equating input energy to output energy. Following assumptions presented in Singh et al. [5], the mathematical modeling can be done as follows:

3.1. Useful energy gain for N similar partially covered PVTFPCs connected in series

As per the study of Singh et al. [5] and Shyam et al. [53], the rate at which useful thermal energy is gained from N number of identical and partially covered PVTFPCs connected in series is given as

$$\dot{Q}_{\mathrm{uN}} = N\left(A_m + A_c\right)\left[\left(\alpha\tau\right)_{\mathrm{eff},N} I\left(t\right) - U_{L,N}\left(T_{\mathrm{fi}} - T_a\right)\right] \tag{1}$$

In the set-up discussed in previous studies, a number (N) of PVTFPCs were connected in series in open loop configuration. While, they have been connected to solar still of single slope type in closed loop in the PVTFPC active solar distillation system considered in the present study. Water coming from the basin of the solar still of single slope type enters the first PVTFPC through DC motor pump and outlet from Nth PVTFPC discharges into the basin of solar still of single slope type. Therefore, T_{fi} turns out to be equal to T_w. The temperature of water coming out from Nth PVTFPC (T_{foN}) is expressed as [53]:

$$T_{\mathrm{foN}} = \frac{\left(AF_R\left(\alpha\tau\right)\right)_1}{\dot{m}_f C_f}\frac{\left(1-K_k^N\right)}{\left(1-K_k\right)} I\left(t\right) + \frac{\left(AF_R U_L\right)_1}{\dot{m}_f C_f}\frac{\left(1-K_k^N\right)}{\left(1-K_k\right)} T_a + K_k^N T_{\mathrm{fi}} \tag{2}$$

where $T_{\mathrm{fi}} = T_w$. The water exiting Nth PVTFPC enters the basin of solar still of single slope type at that temperature. Hence, $T_{\mathrm{wo}} = T_{\mathrm{foN}}$. The expression for the various terms occuring in Eqs. (1) and (2) can be found in Appendix-A.

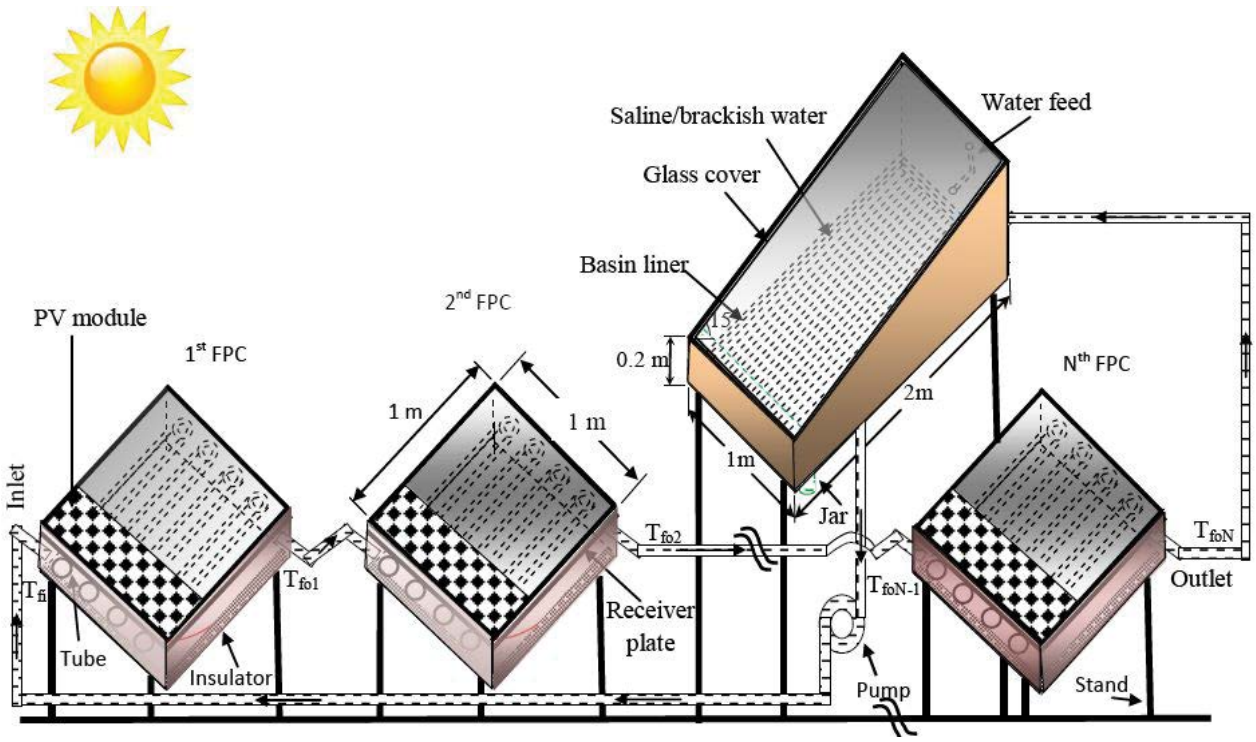

Fig. 1. Schematic diagram of solar still of single slope type integrated with N similar partailly covered PVTFPCs having series connection.

The electrical efficiency of solar cells (η_{cN}) for a number (N) of PVTFPCs as a function of temperature is given as [54,55]:

$$\eta_{cN} = \eta_o\left[1-\beta_o\left(\bar{T}_{cN}-T_o\right)\right] \tag{3}$$

where η_o is the efficiency for a given standard test condition, while $\bar{T}_{cN}$ is the average temperature of the solar cell for the Nth PVTFPC. $\bar{T}_{cN}$ is calculated using the results of Shyam et al. [53] in which $T_{fi} = T_w$ since a number (N) of series connected PVTFPCs are in a closed loop including the basin of solar still of single slope type.

3.2. For solar still of single slope type

The equation based on equating input and output energies for different components of solar still of single slope type can be written and these equations can be further simplified using Eq. (1) following the principle of mathematics and expression for water temperature (T_w) as a function of time can be written as:

$$T_w = \frac{\bar{f}_1(t)}{a_1}\left(1-e^{-a_1 t}\right)+T_{w0}e^{-a_1 t} \tag{4}$$

where T_{w0} is the temperature of water at the initial condition ($t = 0$) and $\bar{f}_1(t)$ is the average value of $f_1(t)$ over the time interval from 0 to t. Once T_w is computed from Eq. (4), one can compute temperature of inner and outer surfaces of glass cover (T_{gi} and T_{go}) as:

$$T_{gi} = \frac{\alpha_g' I_s(t)A_g + h_{1w}T_w A_b + U_{c,ga}T_a A_g}{U_{c,ga}A_g + h_{1w}A_b} \tag{5}$$

$$T_{go} = \frac{\frac{K_g}{L_g}T_{gi} + h_{1g}T_a}{\frac{K_g}{L_g}+h_{1g}} \tag{6}$$

After estimating parameters namely water temperature (T_w) and glass temperatures, the hourly yield ($\dot{m}_{ew}$) can be estimated as:

$$\dot{m}_{ew} = \frac{h_{ewg}A_b\left(T_w - T_{gi}\right)}{L}\times 3{,}600 \tag{7}$$

where L is latent heat which can be taken as 2,400 kJ/kg-K.

4. System analysis at various climates

For the analysis of the effect of dissimilarity of $\dot{m}_f$ and N on yearly overall energy as well exergy for NPVTFPC-SS, 4 climatic situations for each month of year have been taken. These climatic situations can be defined by number of sunshine hours (N') and daily diffuse to daily global irradiation ratio (r') as follows [56].

- Clear day (blue sky) $r' \le 0.25$ and $N' \ge 9$ h
- Hazy day (fully) $0.25 \le r' \le 0.50$ and $7\text{ h} \le N' \le 9\text{ h}$

- Hazy and cloudy (partially) $0.50 \le r' \le 0.75$ and $5\text{ h} \le N' \le 7\text{ h}$
- Cloudy day (fully) $r' \ge 0.75$ and $N' \le 5\text{ h}$

4.1. Energy analysis

The expression of yearly overall energy (E_{out}) for NPVTFPC-SS considering first-law of thermodynamics can be expressed as:

$$E_{out} = \frac{\left(M_{ew} \times L\right)}{3{,}600} + \frac{\left(P_m - P_u\right)}{0.38} \tag{8}$$

where M_{ew} is annual potable water output obtained from NPVTFPC-SS, P_m is yearly electrical power received from PV/T, P_u is yearly electrical power utilized by pump and L is latent heat. Here, factor 0.38 which is present in the denominator converts electrical energy (high grade energy) into heat (low grade energy). This factor is basically the efficacy of power output taken from conventional power plant [57].

The hourly electrical energy ($\dot{E}x_e$) for the solar panel used in NPVTFPC-SS can be expressed as follows:

$$\dot{E}x_e = A_m I_b(t) \sum_{1}^{N} \left(\alpha \tau_g \eta_{cN}\right) \tag{9}$$

Eq. (9) can be used for evaluating daily electrical exergy of type (a) climatic situation by summing the hourly value of 10 h because the solar flux exists for 10 h only. The similar approach has been used to work out the daily electrical energy for rest types of climatic situation, that is, type (b) to type (d). The value of electrical energy on monthly basis for type (a) climatic situation has been evaluated as the multiplication of electrical energy on daily basis and the corresponding value of number of clear days (n'). The similar approach has been used to work out the electrical energy on monthly basis for rest types of climatic situation, that is, type (b) to type (d). The value of net electrical energy on monthly basis has been worked out by summing electrical energies values for type (a) to type (d) climatic situations. The value of electrical energy (P_m) on annual basis has been worked out by the summing of electrical energy on monthly basis for 12 months. The similar approach has been followed for the estimation of annual fresh water yield (M_{ew}).

4.2. Exergy analysis

Exergy analysis has been done based on first-law (energy) and second-law (entropy) of thermodynamics. The hourly output thermal exergy $\dot{E}x_{out}(W)$ for NPVTFPC-SS can be expressed as [58]:

$$\dot{E}x_{out} = h_{ewg} \times \frac{A_b}{2} \times \left[\left(T_w - T_{gi}\right) - \left(T_a + 273\right) \times \ln\left\{\frac{\left(T_w + 273\right)}{\left(T_{gi} + 273\right)}\right\}\right] \tag{10}$$

where

$$h_{ewg} = 16.273 \times 10^{-3} h_{cwg} \left[\frac{P_w - P_{gi}}{T_w - T_{gi}}\right] \text{[59]} \tag{11}$$

$$h_{c,wg} = 0.884 \left[\left(T_w - T_{gi}\right) + \frac{\left(P_w - P_{gi}\right)\left(T_w + 273\right)}{268.9 \times 10^3 - P_w}\right]^{\left(\frac{1}{3}\right)} \text{[60]} \tag{12}$$

$$P_w = \exp\left[25.317 - \frac{5{,}144}{\left(T_w + 273\right)}\right] \tag{13}$$

and

$$P_{gi} = \exp\left[25.317 - \frac{5{,}144}{\left(T_{gi} + 273\right)}\right] \tag{14}$$

Eq. (10) can be used for evaluating daily thermal exergy of type (a) climatic situation by summing the hourly value of 10 h because the solar flux exists for 10 h only. The similar approach has been used to work out the daily thermal exergy for rest types of climatic situation, that is, type (b) to type (d). The value of thermal exergy on monthly basis for type (a) climatic situation has been evaluated as the multiplication of thermal exergy on daily basis and the corresponding value of number of clear days (n'). The similar approach has been used to work out the thermal exergy on monthly basis for rest types of climatic situations, that is, type (b) to type (d). The value of net thermal exergy on monthly basis has been worked out by summing thermal exergy values for type (a) to type (d) climatic situations. The value of thermal exergy on yearly basis has been worked out by the summing thermal exergy on monthly basis for 12 months.

The value of yearly overall annual exergy gain ($G_{ex,annual}$) for NPVTFPC-SS has been expressed as follows:

$$G_{ex,annual} = \text{Ex}_{out} + \left(P_m - P_u\right) \tag{15}$$

5. Methodology

The methodology to investigate the effect of $\dot{m}_f$ and N on the yearly overall energy as well as exergy for NPVTFPC-SS are as follows:

Step I

Taking the value of solar flux on the horizontal plane from IMD located at Pune in India, the value of solar flux on inclined plane has been evaluated using Liu and Jordan formula by computational program in MATLAB. The data for surrounding temperature has been accessed from IMD situated at Pune in India.

Step II

The computation for potable water yielding per hour basis for different values of $\dot{m}_f$ and N has been carried out

with the help of Eq. (7) followed by the computation of potable water yielding on per year basis.

Step III

The computation for exergy based on per hour for different values of $\dot{m}_f$ and N has been carried out with the help of Eq. (10) followed by the calculation for exergy on per year basis.

Step IV

The calculation for gross energy output values at various values of $\dot{m}_f$ for given N have been performed using Eq. (8) followed by calculation for gross energy output on per year basis.

Step V

The calculation for gross exergy output values at various values of $\dot{m}_f$ for given N have been performed using Eq. (15) followed by calculation for gross exergy output on per year basis.

The methodology for investigating the effect of $\dot{m}_f$ and N on the yearly overall energy as well as exergy for NPVTFPC-SS have been revealed as Fig. 2 for better understanding.

6. Results and discussion

The required data and all relevant equations have been fed to computational program written in MATLAB. Data on the horizontal surface has been taken from IMD Pune India. Data on the inclined surface has been evaluated using Liu and Jordan formula with the help of MATLAB-2015a. The output of programme has been presented in Figs. 3–7 and Tables 2–4.

Table 2 represents the computation of yearly fresh water yielding for NPVTFPC-SS at $\dot{m}_f$ = 0.02 kg/s and N = 6. Yearly fresh water yielding for N identical FPCs integrated with SS (NFPC-SS) at $\dot{m}_f$ = 0.02 kg/s and N = 6 has been carried out in the similar fashion. The water depth has been taken as 0.14 m. Similarly, fresh water yielding at other values of $\dot{m}_f$ and N has been evaluated and presented as Fig. 3. It is observed from Fig. 3 that the values of fresh water yielding diminish as the value of $\dot{m}_f$ increases at given N. It happens because water flowing through tubes of collector gets less time to absorb heat at higher value of $\dot{m}_f$. The value of fresh water yielding based on year decreases as the value of $\dot{m}_f$ increases and then it becomes almost constant because after certain value of $\dot{m}_f$, heat absorbed by water is very small as water flowing through tubes does not get time due to increased speed and the system behaves as working in passive mode. It has also been observed from Fig. 3 that the value of fresh water yielding increases as the value of N is enhanced at given value of $\dot{m}_f$ because increase in N results in the addition of more heat at enhanced value of N which further enhances the evaporation rate and hence fresh water yielding gets enhanced with increase in N at given $\dot{m}_f$. The value of fresh water yielding for NFPC-SS is higher than the value of fresh water yielding for NPVTFPC-SS because thermal energy gain of collectors increases in the absence of PV/T and higher amount of heat is added to basin which results in increased fresh water yielding.

Table 1
Specifications of solar still of single slope type integrated with N similar partially covered PVTFPCs having series connection

Component	Specification	Component	Specification
Solar still of single slope type			
Length	2 m	Orientation	South
Width	1 m	Thickness of glass cover	0.004 m
Inclination of glass cover	15°	K_g	0.816 W/m-K
Height of smaller side	0.2 m	Thickness of insulation	0.1 m
Material of body	GRP	Thermal conductivity of insulation	0.166 W/m-K
Material of stand	GI	Cover material	Glass
PVT-FPC collector			
Type and no of collectors	Tube in plate type, N	Aperture area	2 m^2
Receiver area of solar water collector	1.0 m × 1.0 m	Area of module	0.25 m × 1.0 m
Collector plate thickness	0.002	Area of collector	0.75 m × 1.0 m
Thickness of copper tubes	0.00056 m	F'	0.968
Length of each copper tubes	1.0 m	ρ	0.84
K_i ($Wm^{-1} K^{-1}$)	0.166	τ_g	0.95
FF	0.8	α_c	0.9
Thickness of insulation	0.1 m	β_c	0.89
Angle of CPC with horizontal	30°	α_p	0.8
Thickness of toughen glass on FPC	0.004 m	Pipe diameter	0.0125 m
Effective area of collector under glass	0.75 m^2	DC motor rating	12 V, 24 W

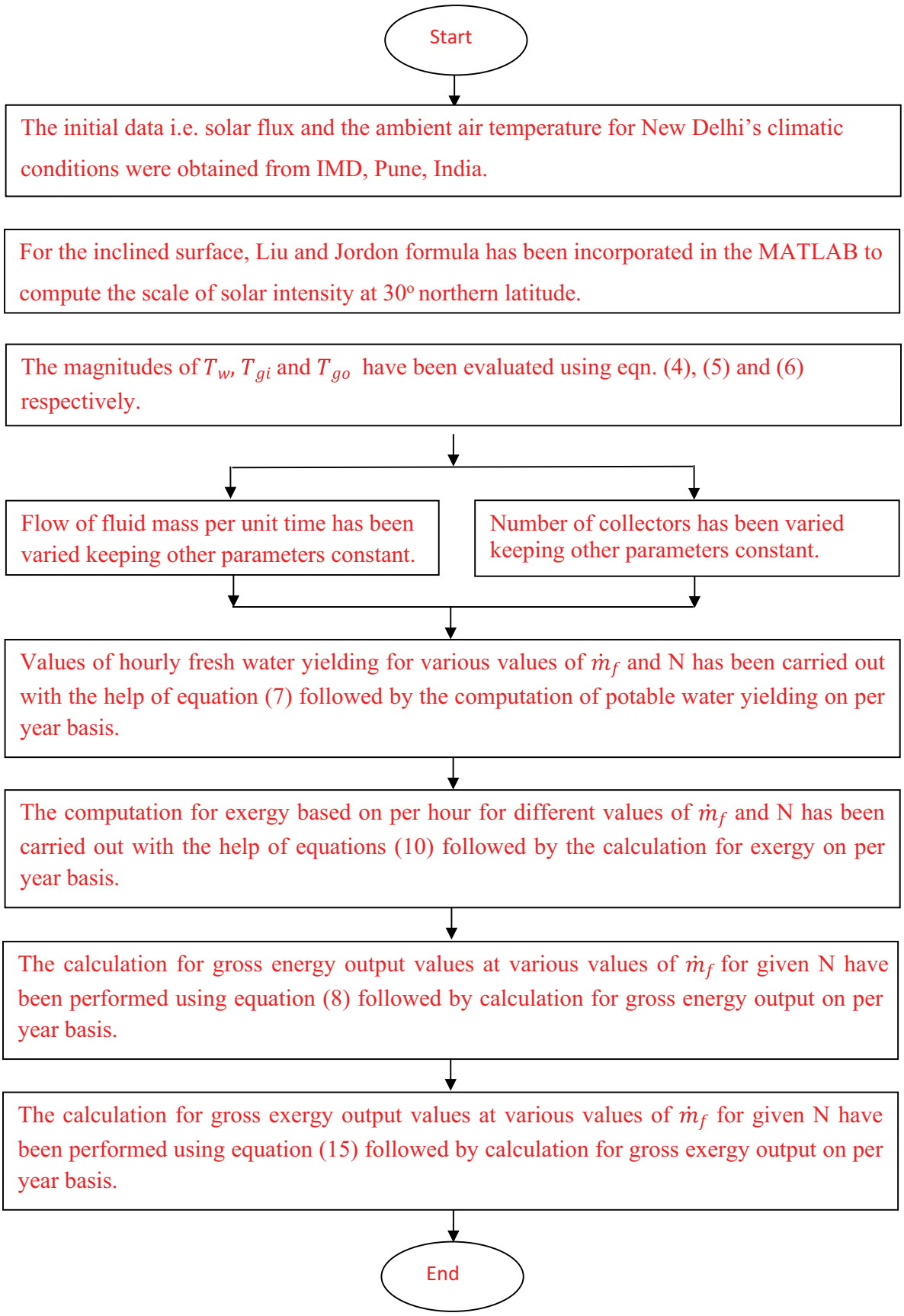

Fig. 2. Flow chart for the methodology followed for NPVTFPC-SS.

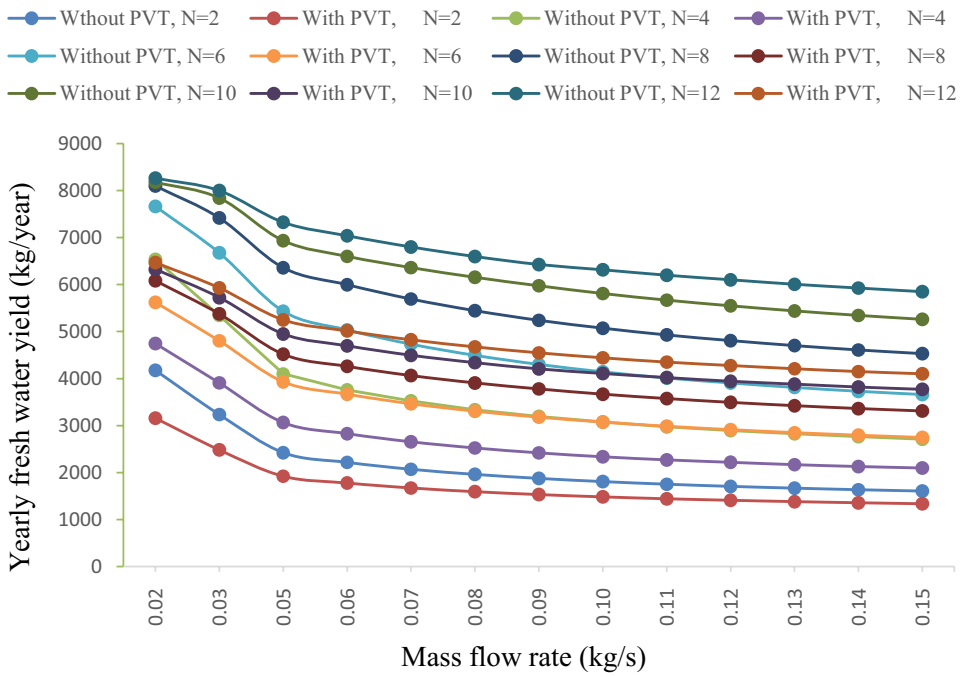

Fig. 3. Variation of yearly fresh water yield with $\dot{m}_f$ for solar still of single slope type integrated with N similar partially covered PVTFPCs at different N.

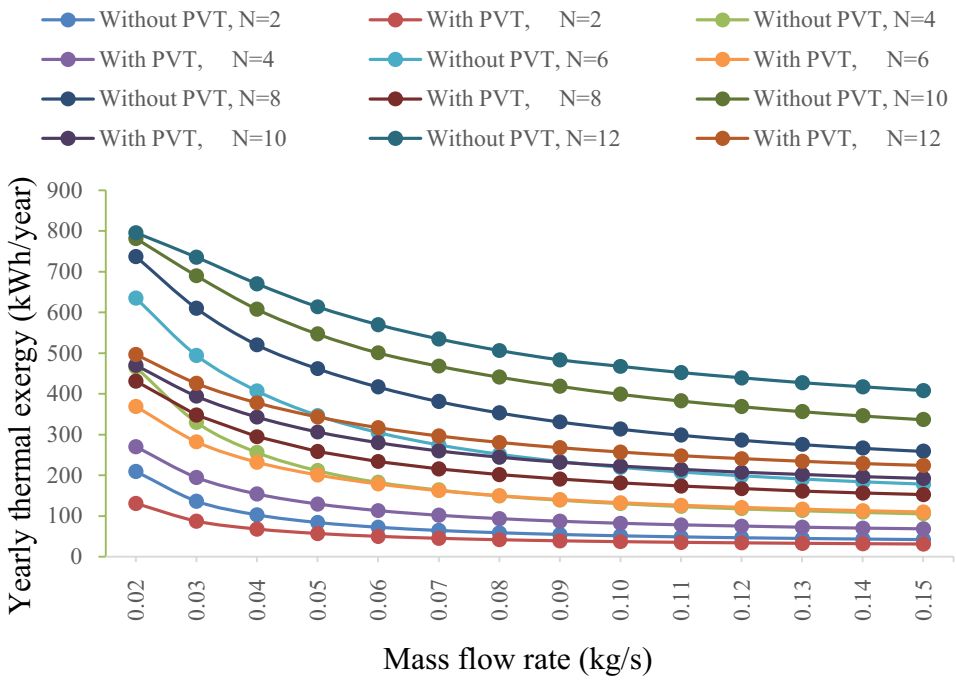

Fig. 4. Variation of yearly thermal exergy with $\dot{m}_f$ for solar still of single slope type integrated with N similar partially covered PVTFPCs at different N.

Table 3 represents the computation of yearly thermal exergy for NPVTFPC-SS at $\dot{m}_f$ = 0.02 kg/s and N = 6. Yearly thermal exergy for NFPC-SS at $\dot{m}_f$ = 0.02 kg/s and N = 6 has been carried out in the similar fashion. The water depth has been taken as 0.14 m. Similarly, thermal exergy at other values of $\dot{m}_f$ has been evaluated and presented as Fig. 4. It is observed from Fig. 4 that the value of thermal exergy decreases as the value of $\dot{m}_f$ increases. It happens because water flowing through tubes of collector gets less time to absorb heat at higher value of $\dot{m}_f$ which result in less rise

Table 2
Computation of yearly fresh water yield for solar still of single slope type integrated with N similar partially covered PVTFPCs at $\dot{m}_f$ = 0.02 kg/s, N = 6 and water depth = 0.14 m

Monthly	Daily yield (kg)	Days (Kind a)	Monthly yield (Kind a) (kg)	Daily yield (kg)	Days (Kind b)	Monthly yield (Kind b) (kg)	Daily yield (kg)	Days (Kind c)	Monthly yield (Kind c) (kg)	Daily yield (kg)	Days (Kind d)	Monthly yield (Kind d) (kg)	Gross monthly yield (kg)
Jan	17.85	3	53.54	16.74	8	133.95	7.33	11	80.67	3.22	9	28.95	297.12
Feb	18.36	3	55.07	18.96	4	75.83	8.32	12	99.88	3.79	9	34.13	264.91
Mar	21.02	5	105.08	23.19	6	139.13	13.02	12	156.28	10.81	8	86.44	486.93
April	23.90	4	95.61	24.84	7	173.89	16.29	14	228.08	16.67	5	83.34	580.93
May	24.27	4	97.07	24.08	9	216.74	22.07	12	264.88	17.70	6	106.20	684.89
June	23.52	3	70.55	24.71	4	98.84	20.76	14	290.61	14.16	9	127.44	587.44
July	21.88	2	43.75	21.86	3	65.58	17.75	10	177.45	12.15	17	206.48	493.26
Aug	20.54	2	41.08	21.58	3	64.73	15.98	7	111.84	11.46	19	217.70	435.34
Sept	24.81	7	173.70	24.21	3	72.63	19.92	10	199.23	12.91	10	129.10	574.66
Oct	22.11	5	110.55	18.81	10	188.08	14.02	13	182.21	8.98	3	26.94	507.78
Nov	19.74	6	118.41	15.45	10	154.51	7.79	12	93.51	7.43	2	14.86	381.30
Dec	20.46	3	61.39	15.50	7	108.52	9.64	13	125.34	4.05	8	32.39	327.64
												Yearly fresh water yield (kg)	5,622.21

Table 3
Computation of yearly thermal exergy for solar still of single slope type integrated with N similar partially covered PVTFPCs at $\dot{m}_f$ = 0.02 kg/s, N = 6 and water depth = 0.14 m

Daily exergy (kWh)	Days (Kind a)	Monthly exergy (Kind a) (kWh)	Daily exergy (kWh)	Days (Kind b)	Monthly exergy (Kind b) (kWh)	Daily exergy (kWh)	Days (Kind c)	Monthly exergy (Kind c) (kWh)	Daily exergy (kWh)	Days (Kind d)	Monthly exergy (Kind d) (kWh)	Gross monthly exergy (kWh)
1.53	3	4.59	1.38	8	11.05	0.38	11	4.18	0.11	9	0.95	20.78
1.46	3	4.39	1.54	4	6.18	0.41	12	4.98	0.12	9	1.09	16.64
1.64	5	8.18	1.94	6	11.62	0.74	12	8.85	0.54	8	4.36	33.01
1.78	4	7.13	1.92	7	13.46	0.91	14	12.68	0.95	5	4.75	38.02
1.69	4	6.75	1.66	9	14.94	1.42	12	16.99	0.95	6	5.71	44.38
1.65	3	4.96	1.81	4	7.22	1.32	14	18.45	0.68	9	6.16	36.79
1.59	2	3.18	1.60	3	4.80	1.11	10	11.08	0.58	17	9.81	28.87
1.58	2	3.16	1.72	3	5.15	1.02	7	7.11	0.59	19	11.12	26.54
2.09	7	14.65	1.99	3	5.98	1.39	10	13.91	0.66	10	6.58	41.12
1.78	5	8.88	1.35	10	13.51	0.82	13	10.64	0.38	3	1.15	34.19
1.71	6	10.24	1.11	10	11.08	0.37	12	4.46	0.35	2	0.69	26.47
1.78	3	5.34	1.19	7	8.32	0.56	13	7.30	0.14	8	1.15	22.11
											Yearly thermal exergy output (kWh)	368.91

in temperature of water. The value of thermal exergy based on year decreases as the value of $\dot{m}_f$ increases and then it becomes almost constant because after certain value of $\dot{m}_f$, heat absorbed by water is very small as water flowing through tubes does not get time due to increased speed and the system behaves as working in passive mode. It has also been observed from Fig. 4 that the value of yearly thermal exergy increases as the value of N is enhanced at given value of $\dot{m}_f$ because increase in N results in the addition of more heat at enhanced value of N which further enhances the temperature of water and hence yearly thermal exergy gets enhanced with increase in N at given $\dot{m}_f$. The value of thermal exergy for NFPC-SS is higher than the value of thermal exergy for NPVTFPC-SS because thermal energy gain of collectors increases in the absence of PV/T and higher amount of heat is added to basin which results in increased temperature of water in the basin and hence higher thermal exergy gain is obtained for NFPC-SS.

Table 4 represents the computation of yearly electrical exergy for NPVTFPC-SS at $\dot{m}_f$ = 0.02 kg/s and N = 6. The water depth has been taken as 0.14 m. Similarly, electrical exergy at other values of $\dot{m}_f$ has been evaluated and presented as Fig. 5. It is observed from Fig. 5 that the value of electrical exergy increases as the value of $\dot{m}_f$ increases. It happens because water flowing through tubes of collector takes away higher amount of heat from PV/T at higher value of $\dot{m}_f$ which results in decrease in temperature of solar cell. Due to decreased temperature rise of solar cell, better efficiency is obtained and hence higher electrical energy output. It is also observed that the value of electrical exergy output becomes almost constant after certain value of $\dot{m}_f$ and then it becomes almost constant. It has been found to occur because water is not able to take away heat from PV/T at very high velocity of water because water does not have time to collect energy from sun. It has also been observed from Fig. 5 that the value of electrical exergy increases as the value of N is enhanced at given value of $\dot{m}_f$ because increase in N results in the addition of heat collection area as well as PV area. The value of electrical energy output for NFPC-SS becomes nil due to the absence of PVT.

Figs. 6 and 7 represent the variation of yearly overall energy and yearly overall exergy respectively with different values of $\dot{m}_f$ and N. It is observed from Fig. 6 that the yearly gross energy decreases as the value of $\dot{m}_f$ increases due to similar variation in yearly fresh water yielding. The variation in yearly yield and yearly electrical exergy is opposite; however, the decrease in yearly fresh water yield overcome the increases in electrical energy with the increase in value of $\dot{m}_f$. Similar variation has been observed in yearly overall thermal exergy. It has also been observed that overall thermal energy and exergy for NFPC-SS is higher than the corresponding values for NPVTFPC-SS because of similar trends in thermal energy and exergy.

7. Conclusions

The analysis for NPVTFPC-SS and NFPC-SS has been done considering all four kinds of atmospheric situations to know the effect of dissimilarities of $\dot{m}_f$ and N on yearly overall energy as well as exergy. Based on the current research study, the following conclusions have been made:

- The value of yearly fresh water yielding as well as thermal exergy has been found to diminish with the increase in value of $\dot{m}_f$ and becomes almost constant beyond 0.10 kg/s; however, they have been found to increase with increase in N at given $\dot{m}_f$ value.
- The value of yearly electrical exergy has been found to increase marginally with the enhancement in $\dot{m}_f$ value and significantly with the enhancement in N value.
- The value of yearly overall energy as well as exergy has been found to diminish with the increase in value of $\dot{m}_f$

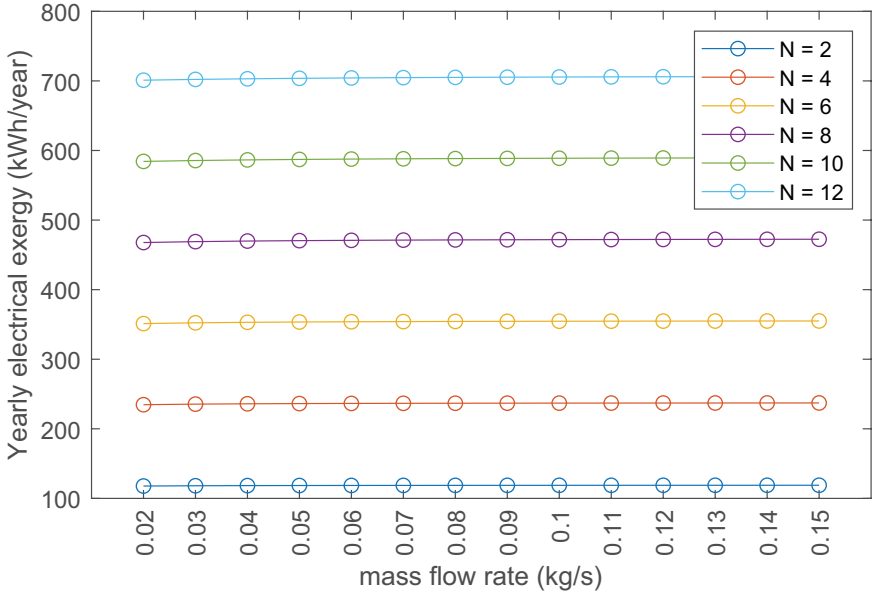

Fig. 5. Variation of yearly electrical exergy with $\dot{m}_f$ for solar still of single slope type integrated with N similar partially covered PVTFPCs at different N.

Table 4
Computation of yearly electrical exergy for solar still of single slope type integrated with N similar partially covered PVTFPCs at $\dot{m}_f$ = 0.02 kg/s, N = 6 and water depth = 0.14 m

Daily exergy (kWh)	Days (Kind a) (kWh)	Monthly exergy (Kind a) (kWh)	Daily exergy (kWh)	Days (Kind b)	Monthly exergy (Kind b) (kWh)	Daily exergy (kWh)	Days (Kind c)	Monthly exergy (Kind c) (kWh)	Daily exergy (kWh)	Days (Kind d)	Monthly exergy (Kind d) (kWh)	Gross monthly exergy (kWh)
1.29	3	3.86	1.24	8	9.89	0.80	11	8.85	0.52	9	4.65	27.24
1.26	3	3.78	1.28	4	5.13	0.83	12	10.00	0.54	9	4.88	23.79
1.23	5	6.16	1.32	6	7.90	0.92	12	11.09	0.83	8	6.60	31.75
1.22	4	4.89	1.26	7	8.85	0.95	14	13.29	0.97	5	4.83	31.86
1.15	4	4.60	1.15	9	10.36	1.08	12	12.95	0.93	6	5.56	33.47
1.18	3	3.55	1.23	4	4.90	1.09	14	15.21	0.84	9	7.58	31.25
1.14	2	2.29	1.16	3	3.48	1.01	10	10.09	0.80	17	13.57	29.42
1.15	2	2.30	1.19	3	3.56	0.98	7	6.85	0.79	19	14.95	27.67
1.24	7	8.69	1.21	3	3.64	1.05	10	10.45	0.77	10	7.68	30.46
1.22	5	6.11	1.11	10	11.10	0.92	13	11.91	0.69	3	2.06	31.19
1.19	6	7.11	1.00	10	9.96	0.66	12	7.97	0.64	2	1.28	26.32
1.24	3	3.72	1.05	7	7.33	0.87	13	11.31	0.55	8	4.44	26.80
									Yearly electrical exergy output (kWh)			351.20

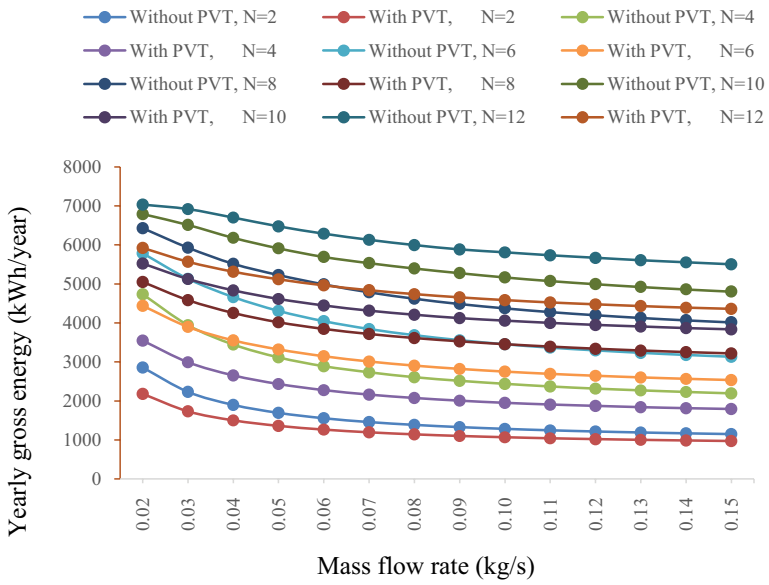

Fig. 6. Variation of yearly gross energy with $\dot{m}_f$ for solar still of single slope type integrated with N similar partially covered PVTFPCs at different N.

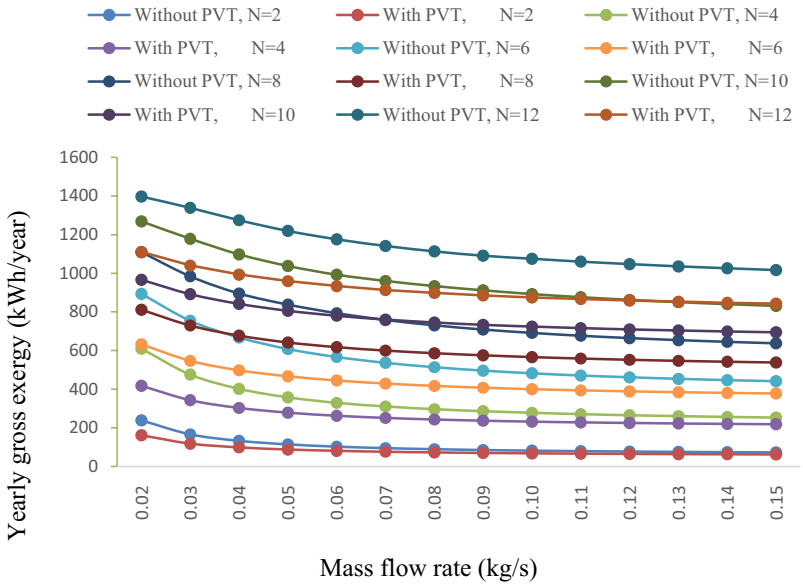

Fig. 7. Variation of yearly gross exergy with $\dot{m}_f$ for solar still of single slope type integrated with N similar partially covered PVTFPCs at different N.

and becomes almost constant beyond 0.10 kg/s; however, they have been found to increase with increase in N at given $\dot{m}_f$ value.

- Values of fresh water yielding, thermal exergy, overall thermal exergy and overall thermal energy is higher for NFPC-SS than the corresponding values for NPVTFPC-SS.

Symbols

A_m — Area covered by PV module, m²
A_c — Area covered by glass, m²
A_g — Area of glass cover, m²
A_b — Area of basin, m²
L — Latent heat, J/kg
L_g — Thickness of glass cover, m
K_g — Thermal conductivity of glass, W/m-K
$I(t)$ — Global radiation falling on collector, W/m²
T_a — Ambient temperature, °C
L_i — Thickness of insulation, m
K_i — Thermal conductivity of insulation, W/m-K
α_c — Absorptivity of the solar cell
$\dot{m}_f$ — Mass flow rate of water, kg/s
τ_g — Transmissivity of the glass, fraction
C_f/C_w — Specific heat of water, J/kg-K

β_0 — Temperature coefficient of efficiency, K^{-1}
L_c — Length of collector covered by glass
L_m — Length of collector covered by PV module
η_c — Solar cell efficiency
η_m — PV module efficiency
η_{cN} — Temperature dependent electrical efficiency of solar cells of a NPVTFPCs
b — Breath of collector, m
$(\alpha\tau)_{eff}$ — Product of effective absorptivity and transmittivity
F' — Collector efficiency factor
T_c — Solar cell temperature, °C
T_p — Absorber plate temperature, °C
L_p — Thickness of absorber plate, m
K_p — Thermal conductivity of absorber plate, W/m-K
T_{fi} — Fluid temperature at collector inlet, °C
T_f — Temperature of fluid in collector, °C
PF_1 — Penalty factor due to the glass covers of module
PF_2 — Penalty factor due to plate below the module
PF_3 — Penalty factor due to the absorption plate for the glazed portion
PF_c — Penalty factor due to the glass covers for the glazed portion
β — Packing factor of the module
η_0 — Efficiency at standard test condition
T_{foN} — Outlet water temperature at the end of Nth PVTFPC water collector, °C
h_i — Heat transfer coefficient for space between the glazing and absorption plate, W/m²-K
h_i' — Heat transfer coefficient from bottom of PVT to ambient, W/m²-K
h_o — Heat transfer coefficient from top of PVT to ambient, W/m²-K
U_{tca} — Overall heat transfer coefficient from cell to ambient, W/m²-K
U_{tcp} — Overall heat transfer coefficient from cell to plate, W/m²-K
h_{pf} — Heat transfer coefficient from blackened plate to fluid, W/m²-K
U_{tpa} — Overall heat transfer coefficient from plate to ambient, W/m²-K
U_{Lm} — Overall heat transfer coefficient from module to ambient, W/m²-K
U_{Lc} — Overall heat transfer coefficient from glazing to ambient, W/m²-K
P_m — Annual power generated from photovoltaic module, kWh
P_u — Annual power utilized by pump, kWh
ϵ — Emissivity
α' — Absorptivity
$\dot{E}x$ — Hourly exergy, W
$I_S(t)$ — Solar intensity on glass cover of solar still of single slope type, W/m²
T_{gi} — Glass temperature at inner surface of glass cover, °C
h_{rwg} — Radiative heat transfer coefficient from water to inner surface of glass cover, W/m²-K
h_{cwg} — Convective heat transfer coefficient from water to inner surface of glass cover, W/m²-K
h_{ewg} — Evaporative heat transfer coefficient, W/m²-K
M_w — Mass of water in basin, kg
$\dot{m}_{ew}$ — Mass of distillate from of double slope solar still, kg
M_{ew} — Annual yield from solar distillation system, kg
a — Clear days, blue sky
b — Hazy days, fully
c — Hazy and cloudy days, partially
d — Cloudy days, fully
$\dot{Q}_{uN}$ — Rate of useful thermal output from N identical partially (25%) covered PVTFPC water collectors connected in series, kWh
$G_{ex,annual}$ — Annual exergy gain, kWh
ln — Natural logarithm
SS — Single slope
T — Time, h
R — Reflectivity
T_s — Temperature of sun, °C
T_w — Temperature of water in basin, °C
T_a — Ambient temperature, °C
T_{wo} — Water temperature at $t = 0$, °C
$\bar{T}_{cN}$ — Average solar cell temperature
E_{out} — Overall annual energy available from PVT-CPC solar distillation system, kWh
Y — Daily yield, kg
M — Monthly yield, kg
Ex — Daily exergy, kWh
Exm — Monthly exergy, kWh
N — Number of PVTFPC water collector
E_{in} — Embodied energy, kWh
FPC — Flat plate collector
PVT — Photovoltaic thermal
N' — Number of sunshine hours
r' — Daily diffuse to daily global irradiation ratio

Subscripts

g — Glass
w — Water
in — Incoming
out — Outgoing
eff — Effective

References

[1] S.N. Rai, G.N. Tiwari, Single basin solar still coupled with flat plate collector, Energy Convers. Manage., 23 (1983) 145–149.
[2] S. Kumar, A. Tiwari, An experimental study of hybrid photovoltaic thermal (PV/T) active solar still, Int. J. Energy Res., 32 (2008) 847–858.
[3] E.C. Kern, M.C. Russell, Combined Photovoltaic and Thermal Hybrid Collector Systems, Proceedings of the 13th IEEE Photovoltaic Specialists, June 5–8, Washington, DC, USA, pp. 1153–1157.
[4] G. Singh, S. Kumar, G.N. Tiwari, Design, fabrication and performance of a hybrid photovoltaic/thermal (PVT) double slope active solar still, Desalination, 277 (2011) 399–406.
[5] D.B. Singh, J.K. Yadav, V.K. Dwivedi, S. Kumar, G.N. Tiwari, I.M. Al-Helal, Experimental studies of active solar still integrated with two hybrid PVT collectors, Sol. Energy, 130 (2016) 207–223.
[6] G.N. Tiwari, J.K. Yadav, D.B. Singh, I.M. Al-Helal, AM. Abdel-Ghany, Exergoeconomic and enviroeconomic analyses of partially covered photovoltaic flat plate collector active solar distillation system, Desalination, 367 (2015) 186–196.

[7] D.B. Singh, G.N. Tiwari, Enhancement in energy metrics of double slope solar still by incorporating N identical PVT collectors, Sol. Energy, 143 (2017) 142–161.
[8] D.B. Singh, Exergoeconomic and enviroeconomic analyses of N identical photovoltaic thermal integrated double slope solar still, Int. J. Exergy, 23 (2017) 347–366.
[9] D.B. Singh, N. Kumar, Harender, S. Kumar, S.K. Sharma, A. Mallick, Effect of depth of water on various efficiencies and productivity of N identical partially covered PVT collectors incorporated single slope solar distiller unit, Desal. Water Treat., 138 (2019) 99–112.
[10] D.B. Singh, Improving the performance of single slope solar still by including N identical PVT collectors, Appl. Therm. Eng., 131 (2018) 167–179.
[11] D.B. Singh, N. Kumar, S. Kumar, V.K. Dwivedi, J.K. Yadav, G.N. Tiwari, Enhancement in exergoeconomic and enviro-economic parameters for single slope solar still by Incorporating N Identical partially covered photovoltaic collectors, J. Sol. Energy Eng., 140 (2018) 051002 (18 pages).
[12] L. Sahota, G.N. Tiwari, Exergoeconomic and enviroeconomic analyses of hybrid double slope solar still loaded with nanofluids, Energy Convers. Manage., 148 (2017) 413–430.
[13] F. Carranza, C. Villa, J. Aguilara, H.A. Borbón-Nuñez, D. Sauceda, Experimental study on the potential of combining TiO_2, ZnO, and Al_2O_3 nanoparticles to improve the performance of a double-slope solar still equipped with saline water preheating, Desal. Water Treat., 216 (2021) 14–33.
[14] M.R. Kouadri, N. Chennouf, M.H. Sellami, M.N. Raache, A. Benarima, The effective behavior of ZnO and CuO during the solar desalination of brackish water in southern Algeria, Desal. Water Treat., 218 (2021) 126–134.
[15] D. Atheaya, A. Tiwari, G.N. Tiwari, I.M. Al-Helal, Analytical characteristic equation for partially covered photovoltaic thermal (PVT) – compound parabolic concentrator (CPC), Sol. Energy, 111 (2015) 176–185.
[16] R. Tripathi, G.N. Tiwari, I.M. Al-Helal, Thermal modelling of N partially covered photovoltaic thermal (PVT)–compound parabolic concentrator (CPC) collectors connected in series, Sol. Energy, 123 (2016) 174–184.
[17] D.B. Singh, G.N. Tiwari, Performance analysis of basin type solar stills integrated with N identical photovoltaic thermal (PVT) compound parabolic concentrator (CPC) collectors: a comparative study, Sol. Energy, 142 (2017) 144–158.
[18] D.B. Singh, G.N. Tiwari, Exergoeconomic, enviroeconomic and productivity analyses of basin type solar stills by incorporating N identical PVT compound parabolic concentrator collectors: a comparative study, Energy Convers. Manage., 135 (2017) 129–147.
[19] D.B. Singh, G.N. Tiwari, Effect of energy matrices on life cycle cost analysis of partially covered photovoltaic compound parabolic concentrator collector active solar distillation system, Desalination, 397 (2016) 75–91.
[20] V.S. Gupta, D.B. Singh, R.K. Mishra, S.K. Sharma, G.N. Tiwari, Development of characteristic equations for PVT-CPC active solar distillation system, Desalination, 445 (2018) 266–279.
[21] V.S. Gupta, D.B. Singh, S.K. Sharma, N. Kumar, T.S. Bhatti, G.N. Tiwari, Modeling self-sustainable fully-covered photo-voltaic thermal-compound parabolic concentrators connected to double slope solar distiller, Desal. Water Treat., 190 (2020) 12–27.
[22] V. Singh, D.B. Singh, N. Kumar, R. Kumar., Effect of number of collectors (N) on life cycle conversion efficiency of single slope solar desalination unit coupled with N identical partly covered compound parabolic concentrator collectors, Mater. Today.: Proc., 28 (2020) 2185–2189.
[23] D.B. Singh, G. Singh, N. Kumar, P.K. Singh, R. Kumar, Effect of mass flow rate on energy payback time of single slope solar desalination unit coupled with N identical compound parabolic concentrator collectors, Mater. Today.: Proc., 28 (2020) 2551–2556.
[24] G.K. Sharma, N. Kumar., D.B. Singh, A. Mallick, Exergoeconoic analysis of single slope solar desalination unit coupled with PVT-CPCs by incorporating the effect of dissimilarity of the rate of flowing fluid mass, Mater. Today.: Proc., 28 (2020) 2364–2368.
[25] H. Prasad, P. Kumar, R.K. Yadav, A. Mallick, N. Kumar, D.B. Singh, Sensitivity analysis of N identical partially covered (50%) PVT compound parabolic concentrator collectors integrated double slope solar distiller unit, Desal. Water Treat., 153 (2019) 54–64.
[26] K. Bharti, S. Manwal, C. Kishore, R.K. Yadav, P. Tiwar, D.B. Singh, Sensitivity analysis of N alike partly covered PVT flat plate collectors integrated double slope solar distiller unit, Desal. Water Treat., 211 (2021) 45–59.
[27] D.B. Singh, Sensitivity analysis of N identical evacuated tubular collectors integrated double slope solar distiller unit by incorporating the effect of exergy, Int. J. Exergy, 34 (2021) 424–447.
[28] K. Sampathkumar, T.V. Arjunan, P. Senthilkumar, The experimental investigation of a solar still coupled with an evacuated tube collector, Energy Sources Part A, 35 (2013) 261–270.
[29] R.V. Singh, S. Kumar, M.M. Hasan, M.E. Khan, G.N. Tiwari, Performance of a solar still integrated with evacuated tube collector in natural mode, Desalination, 318 (2013) 25–33.
[30] S. Kumar, A. Dubey, G.N. Tiwari, A solar still augmented with an evacuated tube collector in forced mode, Desalination, 347 (2014) 15–24.
[31] R.K. Mishra, V. Garg, G.N. Tiwari, Thermal modeling and development of characteristic equations of evacuated tubular collector (ETC), Sol. Energy, 116 (2015) 165–176.
[32] D.B. Singh, V.K. Dwivedi, G.N. Tiwari, N. Kumar, Analytical characteristic equation of N identical evacuated tubular collectors integrated single slope solar still, Desal. Water Treat., 88 (2017) 41–51.
[33] D.B. Singh, G.N. Tiwari, Analytical characteristic equation of N identical evacuated tubular collectors integrated double slope solar still, J. Sol. Energy Eng., 135 (2017) 051003 (11 pages).
[34] D.B. Singh, G.N. Tiwari, Energy, exergy and cost analyses of N identical evacuated tubular collectors integrated basin type solar stills: a comparative study, Sol. Energy, 155 (2017) 829–846.
[35] R.J. Issa, B. Chang, Performance study on evacuated tubular collector coupled solar still in West Texas climate, Int. J. Green Energy, 14 (2017) 793–800.
[36] D.B. Singh, I.M. Al-Helal, Energy metrics analysis of N identical evacuated tubular collectors integrated double slope solar still, Desalination, 432 (2018) 10–22.
[37] D.B. Singh, N. Kumar, A. Raturi, G. Bansal, A. Nirala, N. Sengar, Effect of Flow of Fluid Mass Per Unit Time on Life Cycle Conversion Efficiency of Double Slope Solar Desalination Unit Coupled with N Identical Evacuated Tubular Collectors, Lecture Notes in Mechanical Engineering, Advances in Manufacturing and Industrial Engineering, Select Proceedings of ICAPIE 2019, 2021, pp. 393–402.
[38] S.K. Sharma, D.B. Singh, A. Mallick, S.K. Gupta, Energy metrics and efficiency analyses of double slope solar distiller unit augmented with N identical parabolic concentrator integrated evacuated tubular collectors: a comparative study, Desal. Water Treat., 195 (2020) 40–56.
[39] S.K. Sharma, A. Mallick, S.K. Gupta, N. Kumar, D.B. Singh, G.N. Tiwari, Characteristic equation development for double slope solar distiller unit augmented with N identical parabolic concentrator integrated evacuated tubular collectors, Desal. Water Treat., 187 (2020) 178–194.
[40] R.V. Patel, K. Bharti, G. Singh, R. Kumar, S. Chhabra. D.B. Singh, Solar still performance investigation by incorporating the shape of basin liner: a short review, Mater. Today:. Proc., 43 (2021) 597–604.
[41] R.V. Patel, K. Bharti, G. Singh, G. Mittal, D.B. Singh, A. Yadav, Comparative investigation of double slope solar still by incorporating different types of collectors: a mini review, Mater. Today:. Proc., 38 (2021) 300–304.
[42] R.V. Patel, G. Singh, K. Bharti, R. Kumar, D.B. Singh, A mini review on single slope solar desalination unit augmented with

different types of collectors, Mater. Today:. Proc., 38 (2021) 204–210.
[43] G. Singh, D.B. Singh, S. Kumara, K. Bharti, S. Chhabra, A review of inclusion of nanofluids on the attainment of different types of solar collectors, Mater. Today:. Proc., 38 (2021) 153–159.
[44] G. Bansal, D.B. Singh, C. Kishore, V. Dogra, Effect of absorbing material on the performance of solar still: a mini review, Mater. Today:. Proc., 26 (2020) 1884–1887.
[45] P. Shankar, A. Dubey, S. Kumar, G.N. Tiwari, Production of clean water using ETC integrated solar stills: thermoenviro-economic assessment, Desal. Water Treat., 218 (2021) 106–118.
[46] S. Abdallah, M. Nasir, D. Afaneh, Performance evaluation of spherical and pyramid solar stills with chamber stepwise basin, Desal. Water Treat., 218 (2021) 119–125.
[47] A.K. Thakur, R. Sathyamurthy, S.W. Sharshir, A.E. Kabeel, A.M. Manokar, W. Zhao, An experimental investigation of a water desalination unit using different microparticle-coated absorber plate: yield, thermal, economic, and environmental assessments, Environ. Sci. Pollut. Res., 28 (2021) 37371–37386.
[48] A.K. Thakur, R. Sathyamurthy, R. Velraj, I. Lynch, R. Saidur, A.K. Pandey, S.W. Sharshir, Z. Maf, P.G. Kumarg, A.E. Kabeel, Sea-water desalination using a desalting unit integrated with a parabolic trough collector and activated carbon pellets as energy storage medium, Desalination, 516 (2021) 115217, doi: 10.1016/j.desal.2021.115217.
[49] A.K. Thakur, R. Sathyamurthy, R. Velraj, R. Saidur, J.-Y. Hwange, Augmented performance of solar desalination unit by utilization of nano-silicon coated glass cover for promoting drop-wise condensation, Desalination, 515 (2021) 115191, doi: 10.1016/j.desal.2021.115191.
[50] Z. Said, L.S. Sundar, A.K. Tiwari, H.M. Ali, M. Sheikholeslami, E. Bellos, H. Babar, Recent advances on the fundamental physical phenomena behind stability, dynamic motion, thermophysical properties, heat transport, applications, and challenges of nanofluids, Phys. Rep., (2021), doi: 10.1016/j.physrep.2021.07.002.
[51] Z. Said, A. Amine Hachicha, S. Aberoumand, B.A.A. Yousef, E.T. Sayed, E. Bellose, Recent advances on nanofluids for low to medium temperature solar collectors: energy, exergy, economic analysis and environmental impact, Prog. Energy Combust. Sci., 84 (2021) 100898, doi: 10.1016/j.pecs.2020.100898.
[52] S.K. Sharma, A. Mallick, D.B. Singh, G.N. Tiwari, Experimental study of solar energy-based water purifier of single-slope type by incorporating a number of similar evacuated tubular collectors, Environ. Sci. Pollut. Res., 29 (2022) 6837–6856.
[53] Shyam, G.N. Tiwari, I.M. Al-Helal, Analytical expression of temperature dependent electrical efficiency of N-PVT water collectors connected in series, Sol. Energy, 114 (2015) 61–76.
[54] D.L. Evans, Simplified method for predicting PV array output, Sol. Energy, 27 (1981) 555–560.
[55] T. Schott, Operational Temperatures of PV Modules, Proceedings of 6th PV Solar Energy Conference, 1985, pp. 392–396.
[56] H.N. Singh, G.N. Tiwari, Evaluation of cloudiness/haziness factor for composite climate, Energy, 30 (2005) 1589–1601.
[57] B.J. Huang, T.H. Lin, W.C. Hung, F.S. Sun, Performance evaluation of solar photovoltaic/thermal systems, Sol. Energy, 70 (2001) 443–448.
[58] P.K. Nag, Basic and Applied Thermodynamics, Tata McGraw-Hill, ISBN 0-07-047338-2, 2004.
[59] P.I. Cooper, Digital simulation of experimental solar still data, Sol. Energy, 14 (1973) 451–456.
[60] R.V. Dunkle, Solar Water Distillation, the Roof Type Solar Still and a Multi Effect Diffusion Still, International Developments in Heat Transfer, ASME, Proc. Int. Heat Transfer, Part V, University of Colorado, 1961, p. 895.

Appendix-A

Expressions for various terms used in Eqs. (1)–(9) are as follows:

$$U_{\text{tca}} = \left[\frac{1}{h_o} + \frac{L_g}{K_g}\right]^{-1}; \quad U_{\text{tcp}} = \left[\frac{1}{h_i} + \frac{L_g}{K_g}\right]^{-1};$$

$$h_o = 5.7 + 3.8\text{V}, \quad \text{Wm}^{-2}\text{K}^{-1}; \quad h_i = 5.7, \quad \text{Wm}^{-2}\text{K}^{-1};$$

$$U_{\text{tpa}} = \left[\frac{1}{U_{\text{tca}}} + \frac{1}{U_{\text{tcp}}}\right]^{-1} + \left[\frac{1}{h_i'} + \frac{1}{h_{\text{pf}}} + \frac{L_i}{K_i}\right]^{-1};$$

$$h_i' = 2.8 + 3\text{V}, \quad \text{Wm}^{-2}\text{K}^{-1};$$

$$U_{L1} = \frac{U_{\text{tcp}}U_{\text{tca}}}{U_{\text{tcp}} + U_{\text{tca}}}; \quad U_{L2} = U_{L1} + U_{\text{tpa}};$$

$$U_{\text{Lm}} = \frac{h_{\text{pf}}U_{L2}}{F'h_{\text{pf}} + U_{L2}}; \quad U_{\text{Lc}} = \frac{h_{\text{pf}}U_{\text{tpa}}}{F'h_{\text{pf}} + U_{\text{tpa}}};$$

$$\text{PF}_1 = \frac{U_{\text{tcp}}}{U_{\text{tcp}} + U_{\text{tca}}}; \quad \text{PF}_2 = \frac{h_{\text{pf}}}{F'h_{\text{pf}} + U_{L2}};$$

$$\text{PF}_c = \frac{h_{\text{pf}}}{F'h_{\text{pf}} + U_{\text{tpa}}}; \quad (\alpha\tau)_{\text{1eff}} = (\alpha_c - \eta_c)\tau_g\beta_c;$$

$$(\alpha\tau)_{\text{2eff}} = \alpha_p\tau_g^2(1-\beta_c); \quad (\alpha\tau)_{\text{meff}} = \left[(\alpha\tau)_{\text{2eff}} + \text{PF}_1(\alpha\tau)_{\text{1eff}}\right];$$

$$(\alpha\tau)_{\text{ceff}} = \text{PF}_c \cdot \alpha_p\tau_g; \quad A_m = WL_m; \quad A_c = WL_c;$$

$$A_cF_{\text{Rc}} = \frac{\dot{m}_fC_f}{U_{\text{Lc}}}\left(1 - \exp\left(\frac{-F'U_{\text{Lc}}A_c}{\dot{m}_fc_f}\right)\right);$$

$$A_mF_{\text{Rm}} = \frac{\dot{m}_fC_f}{U_{\text{Lm}}}\left(1 - \exp\left(\frac{-F'U_{\text{Lm}}A_m}{\dot{m}_fC_f}\right)\right);$$

$$\left(AF_R(\alpha\tau)\right)_1 = \left[A_cF_{\text{Rc}}(\alpha\tau)_{\text{ceff}} + \text{PF}_2(\alpha\tau)_{\text{meff}}A_mF_{\text{Rm}}\left(1 - \frac{A_cF_{\text{Rc}}U_{\text{Lc}}}{\dot{m}_fC_f}\right)\right];$$

$$\left(AF_RU_L\right)_1 = \left[A_cF_{\text{Rc}}U_{\text{Lc}} + A_mF_{\text{Rm}}U_{\text{Lm}}\left(1 - \frac{A_cF_{\text{Rc}}U_{\text{Lc}}}{\dot{m}_fC_f}\right)\right];$$

$$K_K = \left(1 - \frac{\left(AF_R U_L\right)_1}{\dot{m}_f c_f}\right); \quad \left(AF_R(\alpha\tau)\right)_{m1} = \mathrm{PF}_2(\alpha\tau)_{\mathrm{meff}} A_m F_{\mathrm{Rm}};$$

$$\left(AF_R U_L\right)_{m1} = A_m F_{\mathrm{Rm}} U_{\mathrm{Lm}}; \quad K_m = \left(1 - \frac{A_m F_{\mathrm{Rm}} U_{\mathrm{Lm}}}{\dot{m}_f C_f}\right);$$

$$(\alpha\tau)_{\mathrm{eff},N} = \frac{\left(AF_R(\alpha\tau)\right)_1}{(A_c + A_m)}\left[\frac{1-(K_K)^N}{N(1-K_K)}\right];$$

$$U_{L,N} = \frac{\left(AF_R U_L\right)_1}{\left(A_c + A_m\right)}\left[\frac{1-(K_K)^N}{N(1-K_K)}\right]$$

$$a_1 = \frac{1}{M_w C_w}\left[\dot{m}_f C_f\left(1 - K_k^N\right) + U_s A_b\right];$$

$$\overline{f}_1(t) = \frac{1}{M_w C_w}\left[\begin{array}{l}\alpha'_{\mathrm{eff}} A_b \overline{I}_s(t) + \frac{\left(1-K_k^N\right)}{\left(1-K_k\right)}\left(AF_R(\alpha\tau)\right)_1 \overline{I}_c(t) + \\ \left(\frac{\left(1-K_k^N\right)}{\left(1-K_k\right)}\left(AF_R U_L\right)_1 + U_s A_b\right)\overline{T}_a\end{array}\right]$$

$$\alpha'_{\mathrm{eff}} = \alpha'_w + h_1\alpha'_b + h'_1\,\alpha'_g; \quad h_1 = \frac{h_{\mathrm{bw}}}{h_{\mathrm{bw}} + h_{\mathrm{ba}}};$$

$$h'_1 = \frac{h_{1w} A_g}{U_{c,\mathrm{ga}} A_g + h_{1w} A_b}; \quad h_{1w} = h_{\mathrm{rwg}} + h_{\mathrm{cwg}} + h_{\mathrm{ewg}};$$

$$h_{\mathrm{ewg}} = 16.273 \times 10^{-3} h_{\mathrm{cwg}}\left[\frac{P_w - P_{\mathrm{gi}}}{T_w - T_{\mathrm{gi}}}\right];$$

$$h_{\mathrm{cwg}} = 0.884\left[\left(T_w - T_{\mathrm{gi}}\right) + \frac{\left(P_w - P_{\mathrm{gi}}\right)\left(T_w + 273\right)}{268.9 \times 10^3 - P_w}\right]^{\frac{1}{3}};$$

$$P_w = \exp\left[25.317 - \frac{5{,}144}{T_w + 273}\right]; \quad P_{\mathrm{gi}} = \exp\left[25.317 - \frac{5{,}144}{T_{\mathrm{gi}} + 273}\right];$$

$$h_{\mathrm{rwg}} = \left(0.82 \times 5.67 \times 10^{-8}\right)\left[\left(T_w + 273\right)^2 + \left(T_{\mathrm{gi}} + 273\right)^2\right]\left[T_w + T_{\mathrm{gi}} + 546\right];$$

$$U_s = U_t + U_b; \quad U_b = \frac{h_{\mathrm{ba}} h_{\mathrm{bw}}}{h_{\mathrm{bw}} + h_{\mathrm{ba}}}; \quad U_t = \frac{h_{1w} U_{c,\mathrm{ga}} A_g}{U_{c,\mathrm{ga}} A_g + h_{1w} A_b};$$

$$U_{c,\mathrm{ga}} = \frac{\frac{K_g}{L_g} h_{1g}}{\frac{K_g}{L_g} + h_{1g}}; \quad h_{\mathrm{ba}} = \left[\frac{L_i}{K_i} + \frac{1}{h_{\mathrm{cb}} + h_{rb}}\right]^{-1};$$

$$h_{\mathrm{cb}} + h_{\mathrm{rb}} = 5.7\,\mathrm{W\,m^{-2}K^{-1}}, \quad h_{\mathrm{bw}} = 250\,\mathrm{W\,m^{-2}K^{-1}};$$